Radiative and Photochemical Processes in Mesospheric Dynamics: Part IV, Stability of a Zonal Vortex at Mid-Latitudes to Baroclinic Waves

RICHARD S. LINDZEN[1]

Harvard University, Cambridge, Mass.

(Manuscript received 25 January 1965)

ABSTRACT

The models developed in Part I for radiative transfer and ozone photochemistry in the mesosphere are incorporated into a two-level model for baroclinic flow, and the effect of radiative and photochemical processes on the stability of the flow is separately investigated for radiative and photochemical conditions obtaining at 30 km and 52.5 km. In each case it is found that the flow is unstable for all non-zero values of shear, in contrast to the adiabatic case where instability required that the shear exceed some critical shear. At 30 km the instabilities at low shears differ considerably from the instabilities for higher shears near the critical shear of the adiabatic theory. The latter have a dominant wavelength of the order of 10,000 km and a phase speed relative to the mean zonal wind of about -20 m sec^{-1}. The former have a dominant wavelength of about 5000 km and a relative phase speed of about -2 m sec^{-1}. The effect of the advection of ozone on the heating appears to be responsible for the low shear mode. This effect is negligible at 52.5 km where there are no significant differences (apart from growth rate) between low and high shear instabilities. The instabilities at this level have a dominant wavelength of about 7900 km and a relative phase speed of about -20 m sec^{-1}.

1. Introduction

In Part III it was shown that radiative and photochemical processes destabilized a baroclinic zonal vortex with respect to axially symmetric disturbances. It was also shown that, in the absence of these processes, the atmosphere is generally stable with respect to such disturbances. In the troposphere such instabilities are not, in fact, observed. It is found, however, that a zonal vortex in the troposphere is generally unstable with respect to baroclinic waves. Such waves differ from the above described disturbances in that their meridional circulations are in geostrophic balance with east-west gradients in the disturbance temperature field.[2] The relative phase of the meridional velocity and temperature in these instabilities results in the conversion of zonal potential energy into kinetic energy. As was pointed out in Part I, this phase relation, and hence the stability properties of the medium, is altered by the action of photochemistry and radiative transfer. How, and to what extent it is altered is studied in this part. Within the context of the model used (two-level), it will be shown that photochemical and radiative processes destabilize a baroclinic medium that would, in terms of adiabatic criteria, be stable. The explicit way in which this is done varies with altitude. At 30 km the important processes are advection of ozone and infrared cooling; at 52.5 km photochemistry is important insofar as it accelerates cooling (see Section 5, Part I).

In view of the cumbersome nature of the mathematical treatment of the baroclinic stability problem in the adiabatic case (*viz.*, Charney, 1947; Kuo, 1953; Burger, 1962), it behooves us to seek out the simplest model exhibiting baroclinic instability. Photochemistry and radiative transfer may then be introduced into such a model, and their effects studied. Since our present purpose is mainly to determine whether photochemistry and radiative transfer can play significant roles in stabilizing or destabilizing a fluid, such a procedure should be adequate. The choice of a hydrodynamic model does, however, involve a difficulty. There is some lack of agreement among detailed treatments of the adiabatic case as to the precise statement of the conditions of instability to baroclinic waves; thus, in contrast to the situation in Part III, we have no explicit criterion for judging the faithfulness of our model to "reality." Fortunately, there exists a very simple model, Phillips' (1956) 2-level model, which when used in a numerical weather simulation experiment, successfully reproduced the atmosphere's behavior, at least with respect to baroclinic waves. This model may be used, less ambitiously, to examine the stability of a model atmosphere to baroclinic waves. This is done, for example, in Thompson (1961), and it is Thompson's approach that we will use.

2. Equations in pressure coordinates

If we adopt the hydrostatic approximation, then our hydrodynamic equations may be conveniently re-

[1] Now at the National Center for Atmosheric Research, Boulder, Colo.

[2] Such gradients are, by definition, zero in axially symmetric disturbances whose meridional circulations arise in order to conserve zonal momentum in the face of a changing thermal wind.

written in terms of pressure coordinates, with p replacing z as an independent variable. The details of this change of variables are given in Thompson (1961). The equations are

$$\left(\frac{\partial \mathbf{v}}{\partial t}\right)_p + u\left(\frac{\partial \mathbf{v}}{\partial x}\right)_p + v\left(\frac{\partial \mathbf{v}}{\partial y}\right)_p + \omega\frac{\partial \mathbf{v}}{\partial p} + \mathbf{k}\times f\mathbf{v} + g\nabla_p z = 0, \quad (1)$$

$$\nabla_p \cdot \mathbf{v} + \frac{\partial \omega}{\partial p} = 0, \quad (2)$$

$$\left(\frac{\partial \Theta}{\partial t}\right)_p + \mathbf{v}\cdot\nabla_p\Theta + \omega\frac{\partial \Theta}{\partial p} = \frac{\Theta}{c_p T}\frac{dq}{dt}, \quad (3)$$

$$\frac{\partial z}{\partial p} = -\frac{\alpha}{g}; \quad \alpha \equiv \frac{1}{\rho}, \quad (4)$$

$$p\alpha = RT, \quad (5)$$

$$\Theta = T\left(\frac{p_0}{p}\right)^{\kappa}, \quad (6)$$

where $\mathbf{v}=u\mathbf{i}+v\mathbf{j}$=horizontal velocity, $\omega=dp/dt$, dq/dt =heating rate per unit volume, Θ=potential temperature, and other variables retain their common meaning. In addition, we have from Part I an expression for dq/dt and an ozone equation:

$$\frac{dq}{dt} = c_p(\eta\varphi - aT + b), \quad (7)$$

and

$$\left(\frac{\partial \varphi}{\partial t}\right)_p + u\left(\frac{\partial \varphi}{\partial x}\right)_p + v\left(\frac{\partial \varphi}{\partial y}\right)_p + \omega\frac{\partial \varphi}{\partial p} = 2\left\{\frac{n_2}{n_m}q_2(y,p) - q_3\frac{1}{n_2}K(T)\varphi^2\right\}, \quad (8)$$

where all quantities are defined in Part I. Eqs. (1) and (2) may be used in order to obtain an equation for the vorticity, $\xi=\partial v/\partial x-\partial u/\partial y$, i.e.,

$$\frac{\partial \xi}{\partial t} + \mathbf{v}\cdot\nabla(\xi+f) - (\xi+f)\frac{\partial \omega}{\partial p} + \omega\frac{\partial \xi}{\partial p} + \hat{\mathbf{k}}\cdot\nabla\omega\times\frac{\partial \mathbf{v}}{\partial p} = 0. \quad (9)$$

Phillips (1963), in an order of magnitude analysis, showed that (9) could be approximated by

$$\nabla^2\frac{\partial z}{\partial t} + J(z, \xi+f) - \frac{f^2}{g}\frac{\partial \omega}{\partial p} = 0, \quad (10)$$

when $\mathrm{Ro}(=V/fL)$, the Rossby number, is small. V is a characteristic horizontal velocity, L, a characteristic horizontal length and J is the Jacobian operator. Consistent with the degree of approximation involved in obtaining (10) we have

$$\mathbf{v} = \mathbf{k}\times\frac{g}{f}\nabla z, \quad (11)$$

and

$$\xi = \frac{g}{f}\nabla^2 z. \quad (12)$$

Ro is typically of the order of 0.1 for motions in the troposphere; it is usually larger in the stratosphere-mesosphere. We will nevertheless take (10) as our equation for vorticity.

From Eqs. (4)–(6) we have

$$\Theta \equiv T\left(\frac{p_0}{p}\right)^{\kappa} = \frac{p}{R\rho}\left(\frac{p_0}{p}\right)^{\kappa} = -\frac{gp}{R}\left(\frac{p_0}{p}\right)^{\kappa}\frac{\partial z}{\partial p}. \quad (13)$$

Using (13) and (11), (3) becomes

$$\frac{\partial}{\partial t}\frac{\partial z}{\partial p} + \frac{g}{f}J\left(z, \frac{\partial z}{\partial p}\right) - \sigma\omega = -\frac{R}{gc_p}\frac{1}{p}\frac{dq}{dt}, \quad (14)$$

where

$$\sigma \equiv \left(\frac{1}{g\rho\Theta}\frac{\partial \Theta}{\partial p}\right).$$

If one writes $\sigma=\sigma_0+\sigma'$, where σ_0 is some time and latitude mean of σ, then one generally finds $\sigma_0 \gg \sigma'$. Hence, it suffices to replace σ in (14) with σ_0;

$$\frac{\partial}{\partial t}\frac{\partial z}{\partial p} + \frac{g}{f}J\left(z, \frac{\partial z}{\partial p}\right) - \sigma_0\omega = -\frac{R}{gc_p}\frac{1}{P}\frac{dq}{dt}. \quad (15)$$

The retention of all the terms in (15) is consistent with our small Ro approximations provided that $\mathrm{Ro}^2\ \mathrm{Ri} \lesssim O(1)$ where

$$\mathrm{Ri} = \frac{R^2T_0\left(\frac{dT_0}{dz}+\frac{g}{c_p}\right)}{gV^2}.$$

$\mathrm{Ri}\doteq 70$ in the troposphere and about 200 in the stratosphere. The condition is, therefore, satisfied in both regions.

Using (13), we may eliminate T from (7) to obtain

$$\frac{dq}{dt} = c_p\left(\eta\varphi + a\frac{g}{R}p\frac{\partial z}{\partial p} + b\right). \quad (16)$$

Using (31) from Part I, as well as (11) and (13), (8) becomes

$$\frac{\partial \varphi}{\partial t} + \frac{g}{f}J(z,\varphi) + \omega\frac{\partial \varphi}{\partial p} = 2\left\{\frac{n_2}{n_m}q_2(y,p) + \frac{q_3 g\rho}{n_2}E\frac{\partial z}{\partial p}\exp\left[\frac{DR}{g\rho}\left(\frac{\partial z}{\partial p}\right)^{-1}\right]\varphi^2\right\}. \quad (17)$$

Eqs. (10), (15), (16) and (17) form a complete set of equations for z, ω and φ. Our procedure will be to assume a basic, irrotational, zonal flow, independent of y, but dependent on p, in geostrophic balance with a radiative-photochemical equilibrium temperature field. For such a flow

$$z_0=-\frac{f}{g}U_0(p)y, \tag{18}$$

$$\omega_0=0, \tag{19}$$

$$\eta\varphi_0+a\frac{g}{R}p\frac{\partial z_0}{\partial p}+b=0, \tag{20}$$

and

$$\frac{n_2}{n_m}q_2(y,p)-q_3\frac{\rho}{n_2}gE\frac{\partial z_0}{\partial p}\exp\left[\frac{DR}{gp_0}\left(\frac{\partial z_0}{\partial p}\right)^{-1}\right]\varphi_0^2=0, \tag{21}$$

where z_0, ω_0, and φ_0 trivially satisfy Eqs. (10) and (15). The satisfaction of (17) turns on the y-dependence of q_2 being such that φ_0 is linear in y as required by (18) and (20). While this is never precisely the case, the physics of our situation is not basically altered by such an assumption. The vertical structure of the fields described by (20) and (21) may be seen in Part I. We now seek to investigate the behavior of small perturbations on the basic field:

$$\begin{aligned}z&=z_0+z'(x,p,t),\\ \omega&=\omega'(x,p,t),\\ \varphi&=\varphi_0+\varphi'(x,p,t).\end{aligned} \tag{22}$$

Note that we have assumed the perturbations to be independent of y (following Rossby, 1939; Charney, 1947; Thompson, 1961; Burger, 1962; and many others); this proves equivalent to ignoring the y-dependence of the coefficients in the equations we are about to develop for the perturbation fields. These equations are obtained by substituting (22) into Eqs. (10), (15), (16) and (17) and retaining only linear (first order) terms in the perturbation quantities [zeroth order terms being eliminated by (18)–(21)]. The details of this procedure for Eqs. (10) and (15) may be found in Thompson (1961), while the procedures for (16) and (17) are analogous to those in Section 5 of Part I. The resulting equations for the perturbations are

$$\frac{\partial}{\partial t}\left(\frac{\partial^2 z'}{\partial x^2}\right)+\beta\frac{\partial z'}{\partial x}+U_0\frac{\partial^3 z'}{\partial x^3}-\frac{f^2}{g}\frac{\partial\omega'}{\partial p}=0, \tag{23}$$

$$\frac{\partial}{\partial t}\left(\frac{\partial z'}{\partial p}\right)+U_0\frac{\partial}{\partial x}\left(\frac{\partial z'}{\partial p}\right)-\frac{dU_0}{dp}\frac{\partial z'}{\partial x}-\sigma_0\omega'=-\frac{R\eta}{g}\psi'-a\frac{\partial z'}{\partial p}, \tag{24}$$

and

$$\frac{\partial\psi'}{\partial t}+\frac{a}{\eta}\frac{g}{R}\frac{dU_0}{dp}\frac{\partial z'}{\partial x}+U_0\frac{\partial\psi'}{\partial x}+\left(\frac{1}{P}\frac{\partial\varphi_0}{\partial p}\right)\omega'=-B(p)\psi'+C(p)\frac{g}{R}\frac{\partial z'}{\partial p}, \tag{25}$$

where

$$\beta=\frac{df}{dy},$$

and

$$\psi'=\frac{\varphi'}{P}.$$

The quantities B, C, η, and a are defined in Part I and η has been taken to be constant. Eqs. (23)–(25) have solutions of the form

$$\begin{Bmatrix}z'\\ \omega'\\ \psi'\end{Bmatrix}=\begin{Bmatrix}\hat{z}'(p)\\ \hat{\omega}'(p)\\ \hat{\psi}'(p)\end{Bmatrix}e^{i\alpha(x-ct)}. \tag{26}$$

Substituting (26) into (23)–(25) we obtain (omitting the caps)

$$i\alpha\{\alpha^2(c-U_0)+\beta\}z'-\frac{f^2}{g}\frac{\partial\omega'}{\partial p}=0, \tag{27}$$

$$i\alpha(c-U_0)\frac{\partial z'}{\partial p}+i\alpha\frac{dU_0}{dp}z'+\sigma_0\omega'=\frac{R\eta}{g}\psi'+a\frac{\partial z'}{\partial p}, \tag{28}$$

and

$$-i\alpha(c-U_0)\psi'+i\alpha\frac{\alpha}{\eta}\frac{g}{R}\frac{dU_0}{dp}z'+\left(\frac{1}{p}\frac{\partial\varphi_0}{\partial p}\right)\omega'=-B(p)\psi'+c(p)\frac{g}{R}\frac{\partial z'}{\partial p}. \tag{29}$$

Eqs. (28) and (29) may be combined in order to eliminate ψ':

$$\mathfrak{A}\frac{\partial z'}{\partial p}+\mathfrak{B}i\alpha\frac{dU_0}{dp}z'+\mathfrak{C}\sigma_0\omega'=0, \tag{30}$$

where

$$\begin{aligned}\mathfrak{A}&=[i\alpha(c-U_0)-B][i\alpha(c-U_0)-a]+\eta C,\\ \mathfrak{B}&=i\alpha(c-U_0)-(a+B),\\ \mathfrak{C}&=i\alpha(c-U_0)-(\chi+B),\end{aligned}$$

and

$$\chi=\frac{R\eta}{\sigma_0 gp}\frac{\partial\varphi_0}{\partial p}.$$

We now have two linear, homogeneous equations for ω' and z', (27) and (30), from which we may obtain a dispersion relation relating c to U_0, dU_0/dp, and the various photochemical and radiative parameters.

3. Two-level model

The coefficients in Eqs. (27) and (30) are functions of p, and this in turn, makes the analytical solution of these equations a very difficult matter [*viz.*, Kuo (1953) for the adiabatic case]. An alternative is the use of a numerical method such as finite differences—of which method the two level model is an example. Following Thompson (1961) we will use this method in our investigation.

In the two-level model, our domain is bounded by $p=p_2=0$ and $p=p_0$. The domain is then divided into four layers, separated by the levels $p=p_{\frac{3}{4}}=\frac{3}{4}p_0$, $p=p_1=\frac{1}{2}p_0$ and $p=p_{\frac{1}{4}}=\frac{1}{4}p_0$. Eq. (27) is applied at the levels $p_{\frac{1}{4}}$ and $p_{\frac{3}{4}}$, while Eq. (30) is applied at the level p_1. Vertical derivatives are approximated by finite differences. Thus

$$\left(\frac{\partial\omega'}{\partial p}\right)_{\frac{1}{4}}\doteq\frac{\omega_0-\omega_1}{\Delta p}, \tag{31}$$

$$\left(\frac{\partial\omega'}{\partial p}\right)_{\frac{3}{4}}\doteq\frac{\omega_1-\omega_2}{\Delta p}, \tag{32}$$

and

$$\left(\frac{\partial z'}{\partial p}\right)_1\doteq\frac{z_{\frac{1}{4}}'-z_{\frac{3}{4}}'}{\partial p}; \tag{33}$$

also

$$z_1'\doteq\frac{z_{\frac{1}{4}}'+z_{\frac{3}{4}}'}{2}. \tag{34}$$

A similar procedure is used for the basic fields; i.e.,

$$(U_0)_1=U_1=\tfrac{1}{2}(U_{\frac{1}{4}}+U_{\frac{3}{4}}), \tag{35}$$

and

$$\left(\frac{dU_0}{dp}\right)_1\doteq\frac{1}{\Delta p}(U_{\frac{1}{4}}-U_{\frac{3}{4}}), \tag{36}$$

where subscripts have been used to indicate level and $\Delta p=\frac{1}{2}p_0$.

As boundary conditions we will take $\omega'=0$ at $p=p_0$ and at $p=p_2$, thus excluding forced oscillations among other things. The treatment of a section of the mesosphere as being a region bounded below is not entirely realistic. There is, however, evidence that certain disturbances in the mesosphere are independent of conditions immediately below. Moreover, $\omega'=0$ at p_0 is the simplest, readily interpretable boundary condition we could adopt, and furthermore, it permits us to isolate the effects of radiative transfer and photochemistry in a situation whose adiabatic properties are fairly well known.

Proceeding as outlined above, we apply (27) at $p_{\frac{1}{4}}$ and $p_{\frac{3}{4}}$, obtaining

$$i\alpha\{\alpha^2(c-U_{\frac{1}{4}})+\beta\}z_{\frac{1}{4}}'+\frac{f^2}{g}\frac{\omega_1}{\Delta p}=0, \tag{37}$$

and

$$i\alpha\{\alpha^2(c-U_{\frac{3}{4}})+\beta\}z_{\frac{3}{4}}'-\frac{f^2}{g}\frac{\omega_1}{\Delta p}=0. \tag{38}$$

Applying (30) at p_1 we obtain

$$\mathfrak{A}(\alpha,c,p_1)\frac{z_{\frac{1}{4}}'-z_{\frac{3}{4}}'}{\Delta p}+i\alpha\frac{U_{\frac{1}{4}}-U_{\frac{3}{4}}}{\Delta p}\mathfrak{B}(\alpha,c,p_1)\frac{z_{\frac{1}{4}}'+z_{\frac{3}{4}}'}{2}+\sigma_0\mathfrak{C}(\alpha,c,p_1)\omega_1'=0. \tag{39}$$

Eqs. (37)–(39) may be combined to yield

$$(\alpha^2\xi+\beta)\bar{z}-\alpha^2U^*z^*=0, \tag{40}$$

and

$$\left\{(\alpha^2\xi+\beta)-i\frac{\mu^2}{\alpha}\frac{\mathfrak{A}_1}{\mathfrak{C}_1}\right\}z^*+U^*\left\{-\alpha^2+\mu^2\frac{\mathfrak{B}_1}{\mathfrak{C}_1}\right\}=0, \tag{41}$$

where

$$\xi=c-\bar{U},$$

$$\mu^2=-2f^2/\sigma_0g(\Delta p)^2,$$

$$\begin{Bmatrix}\bar{U}\\ \bar{z}\end{Bmatrix}=\frac{1}{2}\begin{Bmatrix}U_{\frac{1}{4}}+U_{\frac{3}{4}}\\ z_{\frac{1}{4}}'+z_{\frac{3}{4}}'\end{Bmatrix},$$

$$\begin{Bmatrix}U^*\\ z^*\end{Bmatrix}=\frac{1}{2}\begin{Bmatrix}U_{\frac{1}{4}}-U_{\frac{3}{4}}\\ z_{\frac{1}{4}}'-z_{\frac{3}{4}}'\end{Bmatrix},$$

and

$$\mathfrak{A}_1=\mathfrak{A}(\alpha,c,p_1)=\{i\alpha\xi-B(p_1)\}(i\alpha\xi-a)+\eta C(p_1),$$
$$\mathfrak{B}_1=\mathfrak{B}(\alpha,c,p_1)=i\alpha\xi-\{a+B(p_1)\},$$

and

$$\mathfrak{C}_1=\mathfrak{C}(\alpha,c,p_1)=i\alpha\xi-\{\chi(p_1)+B(p_1)\}.$$

In order for (40) and (41) to have a non-zero solution, the following must be satisfied:

$$\begin{vmatrix}\alpha^2\xi+\beta & -\alpha^2U^*\\ U^*\left[-\alpha^2+\mu^2\dfrac{\mathfrak{B}_1}{\mathfrak{C}_1}\right] & \left((\alpha^2\xi+\beta)-i\dfrac{\mu^2}{\alpha}\dfrac{\mathfrak{A}_1}{\mathfrak{C}_1}\right)\end{vmatrix}=0,$$

or

$$\begin{aligned}i\alpha\xi\{&\alpha^2(\mu^2+\alpha^2)\xi^2+\beta(2\alpha^2+\mu^2)\xi+[\beta^2+\alpha^2U^{*2}(\mu^2-\alpha^2)]\}\\ &=\alpha^2[\alpha^2(B_1+\chi_1)+\mu^2(B_1+a)]\xi^2\\ &\quad+[2\alpha^2\beta(B_1+\chi_1)+i\mu^2\alpha(aB_1+\eta c_1)+\mu^2\beta(a+B_1)]\xi\\ &\quad+\Big[\beta^2(B_1+\chi_1)+i\frac{\mu^2}{\alpha}\beta(aB_1+\eta c_1)\\ &\qquad+\alpha^2U^{*2}\{\mu^2(B_1+a)-\alpha^2(B_1+\chi_1)\}\Big].\end{aligned} \tag{42}$$

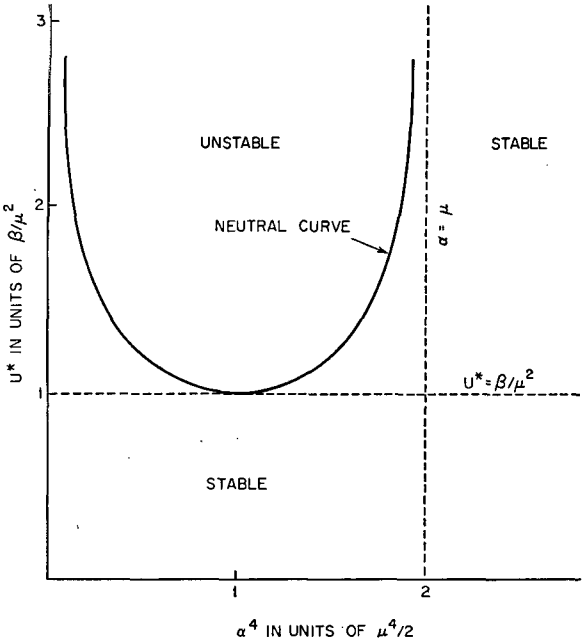

FIG. 1. Adiabatic stability of two-level baroclinic flow. The curve separating unstable solutions from neutrally stable solutions is shown as a function of shear (proportional to U^*) and wavenumber, α. After Thompson (1961).

4. Adiabatic case

In the absence of photochemistry and radiative transfer $a=B=C=\eta=0$, and only the left hand side of (42) remains. This is the case Thompson (1961) treats. With the right hand side of (42) equal to zero, there are three solutions for ξ, i.e.,

$$\xi=0, \tag{43}$$

and

$$\xi=-\frac{\beta(2\alpha^2+\mu^2)}{2\alpha^2(\alpha^2+\mu^2)}\pm\sqrt{\delta}, \tag{44}$$

where

$$\delta=\frac{\beta^2\mu^4}{4\alpha^4(\alpha^2+\mu^2)^2}-U^{*2}\frac{\mu^2-\alpha^2}{\mu^2+\alpha^2}.$$

Only solutions (44) are non-trivial. When δ is positive, ξ is real and neither solution grows with time (we shall refer to such solutions as neutrally stable). However, when δ is negative one of solutions (44) will have a positive imaginary part, and this, in turn, implies that this solution corresponds to a disturbance growing exponentially with time. Hence, the curve $\delta=0$ marks the boundary between unstable and neutrally stable solutions. This curve is shown in Fig. 1. The flow is neutrally stable when $U^*<\beta/\mu^2$. Note that if we were on a constant f-plane where $\beta=0$, then all baroclinic flows would be unstable and baroclinic waves would travel with the mean speed of the basic flow; these results are in agreement with Eady's (1949) work on the stability of baroclinic flow on an f-plane.

5. Non-adiabatic case

The solution of (42) in this case is facilitated by the following change of variables:

$$\tilde{\alpha}=\alpha u^{-1}(2^{\frac{1}{2}}), \tag{45}$$

$$(\tilde{\xi},\tilde{U})=(\xi,U^*)u^2\beta^{-1}, \tag{49}$$

and

$$(\tilde{B}_1,\tilde{a},\tilde{C}_1,\tilde{\eta}_1,\tilde{\chi}_1)=u\beta^{-1}(B_1,a,C_1,\eta,\chi_1). \tag{47}$$

Eq. (42) then becomes

$$\frac{\tilde{\alpha}^2}{\sqrt{2}}\left(1+\frac{\tilde{\alpha}^2}{\sqrt{2}}\right)\tilde{\xi}^2+(1+\sqrt{2}\tilde{\alpha}^2)\tilde{\xi}+\left[1+\frac{\tilde{\alpha}^2}{\sqrt{2}}\tilde{U}^2\left(1-\frac{\tilde{\alpha}^2}{\sqrt{2}}\right)\right]$$
$$=-i\left\{(2^{-\frac{1}{2}})\tilde{\alpha}\left[\frac{\tilde{\alpha}^2}{\sqrt{2}}(\tilde{B}_1+\tilde{\chi}_1)+(\tilde{B}_1+\tilde{a})\right]\tilde{\xi}+\left[\left[\tilde{\alpha}(2^{\frac{1}{2}})(\tilde{B}_1+\tilde{\chi}_1)+\frac{(2^{\frac{1}{2}})}{\tilde{\alpha}}(\tilde{a}+\tilde{B}_1)\right]+i(\tilde{a}\tilde{B}_1+\tilde{\eta}C_1)\right]\right.$$
$$\left.+\left[\left[\frac{(2^{\frac{1}{2}})}{\tilde{\alpha}}(\tilde{B}_1+\tilde{\chi}_1)+\tilde{\alpha}(2^{-\frac{1}{2}})\tilde{U}^2\left((\tilde{B}_1+\tilde{a})-\frac{\tilde{\alpha}^2}{\sqrt{2}}(\tilde{B}_1+\tilde{\chi}_1)\right)\right]+i\frac{\sqrt{2}}{\tilde{\alpha}^2}(\tilde{a}\tilde{B}_1+\tilde{\eta}\tilde{C}_1)\right]\frac{1}{\tilde{\xi}}\right\}, \tag{48}$$

or

$$f(\tilde{\xi})=\mathcal{P}(\tilde{\alpha})\tilde{\xi}^2+\mathcal{Q}(\tilde{\alpha})\tilde{\xi}+\mathcal{R}(\tilde{\alpha},\tilde{U})$$
$$+i\{\mathcal{S}(\tilde{\alpha},\tilde{B}_1,\tilde{\chi}_1,\tilde{a})\tilde{\xi}$$
$$+[\mathcal{T}(\tilde{\alpha},\tilde{B}_1,\tilde{\chi}_1,\tilde{a})+i\mathcal{W}(\tilde{\alpha},\tilde{B}_1,\tilde{C}_1,\tilde{\eta})]$$
$$+[\mathcal{U}(\tilde{\alpha},\tilde{U},\tilde{a},\tilde{B}_1,\tilde{\chi}_1)+i\mathcal{V}(\tilde{a},\tilde{B}_1,\tilde{C}_1,\tilde{\eta},\tilde{\alpha})]\tilde{\xi}^{-1}\}=0, \tag{49}$$

where the definitions of $\mathcal{P}$, $\mathcal{Q}$, $\mathcal{R}$, $\mathcal{S}$, $\mathcal{T}$, $\mathcal{W}$, $\mathcal{U}$, and $\mathcal{V}$ are obvious. The only external parameters in (49) are the photochemical and radiative parameters, $\tilde{a}$, $\tilde{B}_1$, $\tilde{C}_1$, $\tilde{\eta}_1$ and $\tilde{\chi}_1$, which also depend on β and μ. Our procedure will be to obtain, for a given choice of $\tilde{a}_1$, $\tilde{B}_1$, $\tilde{C}_1$, $\tilde{\eta}$, and $\tilde{\chi}_1$, $\tilde{\xi}$ (non-dimensional wave speed relative to mean flow) as a function of $\tilde{\alpha}$ (non-dimensional wave number) and $\tilde{U}^2$ (square of non-dimensional velocity difference between levels $\frac{3}{2}$ and $\frac{1}{2}$). If we choose our photochemical and radiative parambers, a, B, C, η and χ, to be those corresponding to equilibrium at a level where $p=p_1$, then Δp will equal p_1 and knowing Δp, we may compute μ and hence $\tilde{a}_1$, $\tilde{B}_1$, $\tilde{C}_1$, $\tilde{\eta}_1$ and $\tilde{\chi}_1$. This procedure has been followed for $p_1=11.5$ mb ($\sim$30 km) and $p_1=0.5$ mb ($\sim$52.5 km). The equilibrium fields are obtained from the results given in Part I. The method used in

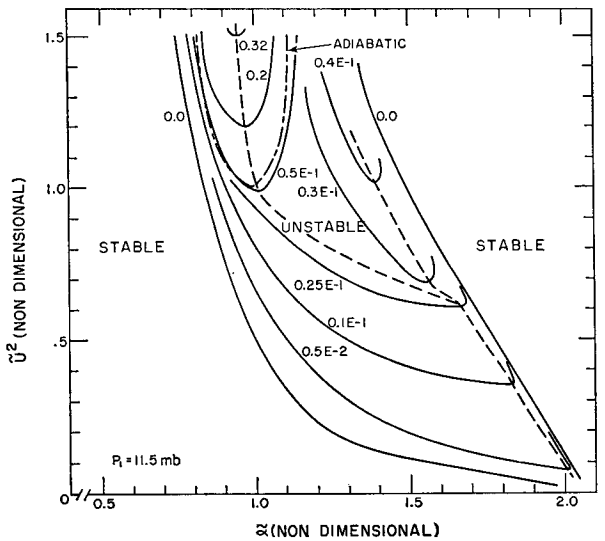

FIG. 2. The stability of two-level baroclinic, radiative, photochemical flow centered at 30 km. $\mathrm{Im}(\tilde{\xi})$ is shown as a function of $\tilde{U}^2$ and $\tilde{\alpha}$ (see text for definitions). Positive $\mathrm{Im}(\tilde{\xi})$ implies instability. The broken lines represent ridges of maximum $\mathrm{Im}(\tilde{\xi})$. Unbroken curves are curves of constant $\mathrm{Im}(\tilde{\xi})$ and are labelled with the values of $\mathrm{Im}(\tilde{\xi})$. The long-short broken curve represents the boundary between neutral and unstable waves for the adiabatic case.

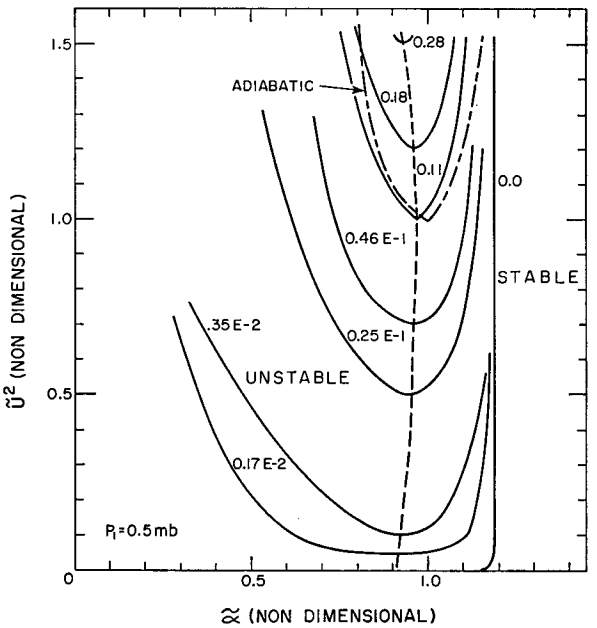

FIG. 3. The stability of two-level, radiative, photochemical flow centered at 52.5 km. $\mathrm{Im}(\tilde{\xi})$ is shown as a function of $\tilde{U}^2$ and $\tilde{\alpha}$ (see text for definitions). Positive $\mathrm{Im}(\tilde{\xi})$ implies instability. The broken lines represent ridges of maximum $\mathrm{Im}(\xi)$. Unbroken curves are curves of constant $\mathrm{Im}(\tilde{\xi})$ and are labelled with the values of $\mathrm{Im}(\tilde{\xi})$. The long-short broken curves represents the boundary between neutral and unstable waves for the adiabatic case.

solving (49) was a modified form of Newton's method (Householder, 1953) whose details may be found in the author's thesis (Lindzen, 1964).

One obtains, in solving (49), three solutions for $\tilde{\xi}$; two always have negative imaginary parts, and therefore correspond to exponentially decaying disturbances, while one, for certain ranges of $\tilde{\alpha}$ and $\tilde{U}$, has a positive

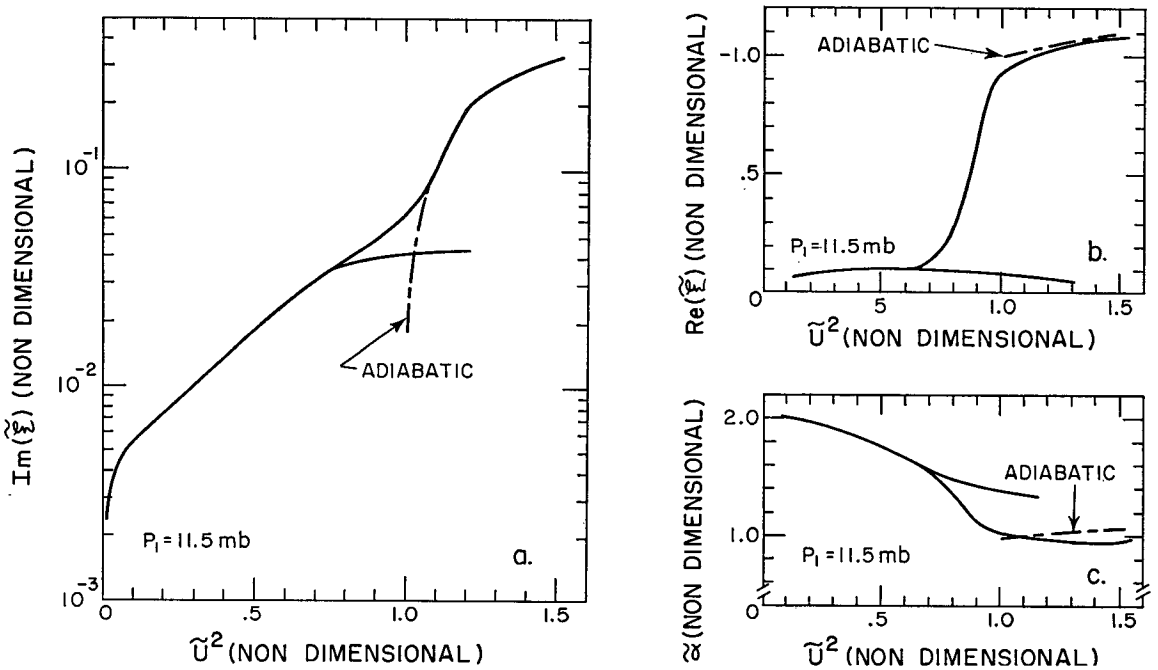

FIG. 4. Growth rates, velocities and wave numbers of disturbances, as a function of wind shear at 30 km; (a) maximum $\mathrm{Im}(\tilde{\xi})$ vs. $\tilde{U}^2$, (b) $\mathrm{Re}(\tilde{\xi})$ vs. $\tilde{U}^2$ at maximum $\mathrm{Im}(\tilde{\xi})$, (c) $\tilde{\alpha}$ vs. $\tilde{U}^2$ at maximum $\mathrm{Im}(\tilde{\xi})$.

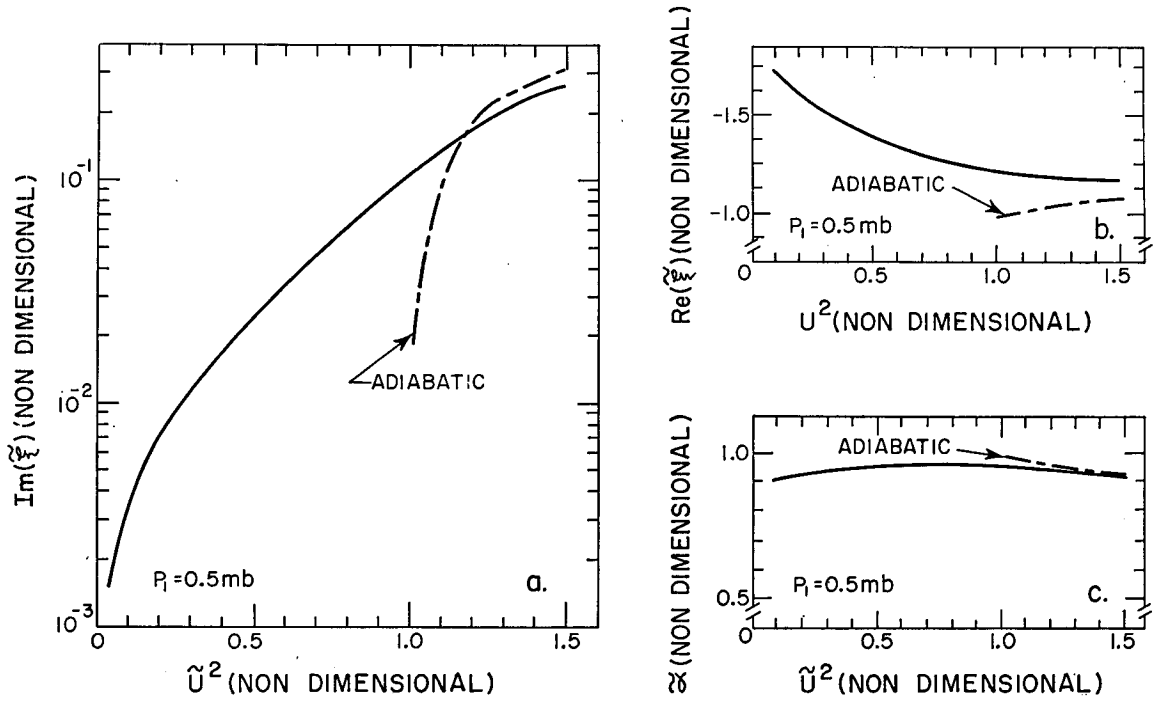

FIG. 5. Growth rates, velocities and wave numbers of disturbances, as a function of wind shear at 52.5 km; (a) maximum Im($\tilde{\xi}$) vs. $\tilde{U}^2$, (b) Re($\tilde{\xi}$) vs. $\tilde{U}^2$ at maximum Im($\tilde{\xi}$), (c) $\tilde{\alpha}$ vs. $\tilde{U}^2$ at maximum Im($\tilde{\xi}$).

imaginary part, corresponding to an unstable disturbance. It is the last which interests us here. The solution of (49) has been carried out in terms of the non-dimensional quantities $\tilde{\xi}$, $\tilde{\alpha}$, and $\tilde{U}$. The results in terms of these quantities for $p_1=11.5$ mb are given in Figs. 2 and 4; the results for $p_1=0.5$ mb are given in Figs. 3 and 5. The non-dimensional quantities are related to dimensional quantities by Eqs. (45) and (46) with the conversion factors being listed in Table 1. In connection with the conversion to dimensional quantities, it proves useful to relate U^* to shear. We have used the following approximation

$$\left(\frac{\overline{dU}}{dz}\right)\doteq\frac{U_{\frac{1}{2}}-U_{\frac{3}{2}}}{z_{0\frac{1}{2}}-z_{0\frac{3}{2}}}=\frac{2U^*}{z_{\frac{1}{2}}-z_{\frac{3}{2}}}.$$

In general $p_{\frac{1}{2}}=3p_{\frac{3}{2}}$, and such isobaric surfaces are separated by about 7 km in the regions we are dealing with. Hence

$$\left(\frac{\overline{dU}}{dz}\right)\doteq\frac{2U^*}{7\text{ km}}. \tag{50}$$

TABLE 1. Values of dimensional factors in Eqs. (45) and (46).

Altitude (km)	μ (km^{-1})	β/μ^2 (km sec^{-1})	$\mu/(2)^{\frac{1}{2}}$ (km^{-1})	β/μ (sec^{-1})
30	0.8×10^{-3}	2.5×10^{-2}	6.7×10^{-4}	2.0×10^{-5}
52.5	1.0×10^{-3}	1.6×10^{-2}	8.3×10^{-4}	1.6×10^{-5}

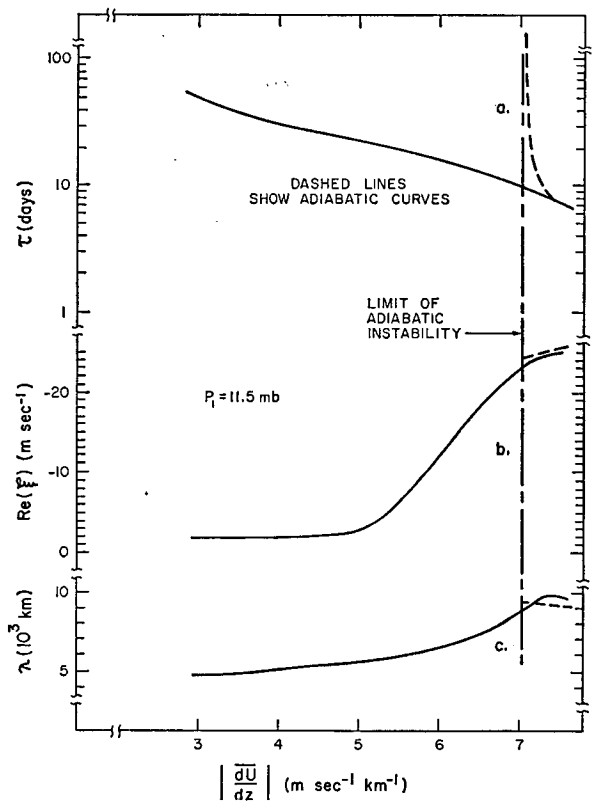

FIG. 6. Time for growth, phase speed and wavelength of most unstable waves as a function of shear at 30 km; (a) time scale, τ, in days, (b) relative phase speed, Re(ξ), m sec^{-1}, (c) wavelength λ, 10^3 km.

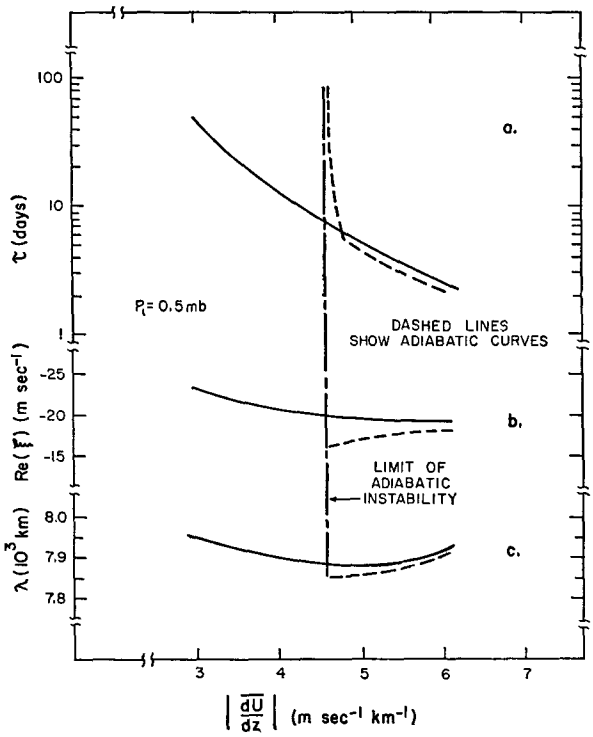

FIG. 7. Time for growth, phase speed and wavelength of most unstable waves as a function of shear at 52.5 km; (a) time scale, τ, in days, (b) relative phase speed, Re(ξ), m sec^{-1}, (c) wavelength λ, 10^3 km.

Certain important aspects of our solutions are shown in terms of dimensional quantities in Figs. 6 and 7 for $p_1=11.5$ mb and $p_1=0.5$ mb, respectively.

In Figs. 2 and 3 we have shown curves of constant Im(ξ) on a $\tilde{U}^2-\tilde{\alpha}$ plane. Positive Im(ξ) is associated with instability. Note that the presence of photochemistry and radiative transfer lead to unstable modes at all values of $\tilde{U}^2$ in contrast to the adiabatic situation shown in Fig. 1 where instability occurs only when $\tilde{U}^2>1$. The boundary between neutrally stable and unstable solutions in the adiabatic case is shown by long-short dashed curves in Figs. 2 and 3. Although instability now exists for all values of $\tilde{U}^2$, small values of $\tilde{U}^2$ are associated with small growth rates. The growth rate is proportional to ($\tilde{\alpha}\xi$). However, at a given value of $\tilde{U}$, ξ varies rapidly with $\tilde{\alpha}$ and hence, the dashed lines in Figs. 2 and 3, representing ridges of maximum Im(ξ), are also approximately ridges of maximum growth rate. The marked differences between Figs. 2 and 3 deserve some comment. Not surprisingly, the physical situations at 11.5 mb and at 0.5 mb are also markedly different. In Table 2 the value of $\tilde{a}$, $\tilde{B}$, $\tilde{\chi}$ and ($\tilde{a}\tilde{B}+\tilde{\eta}\tilde{C}$) at 11.5 mb and at 0.5 mb are listed. They are computed from information in Part I; additional details are given in Lindzen (1964). At 11.5 mb, $\tilde{a}$, $\tilde{B}$ and $\tilde{\chi}$ are of the same order of magnitude ($\tilde{\chi}$ measures the importance of ozone advection to the heating where large $\tilde{\chi}$ is associated with steep vertical gradients in the ozone mixing ratio);

TABLE 2. Photochemical and radiative parameters. $\tilde{a}$, $\tilde{B}$ and $\tilde{\chi}$ are non-dimensionalized according to (β/μ); ($\tilde{a}\tilde{B}+\tilde{\eta}\tilde{C}$) non-dimensionalized according to $(\beta/\mu)^2$.

Altitude (km)	$\tilde{a}$	$\tilde{B}$	$\tilde{\chi}$	$\tilde{a}\tilde{B}+\tilde{\eta}\tilde{C}$
30.0	2.6×10^{-2}	1.8×10^{-2}	1.0×10^{-2}	1.2×10^{-3}
52.5	4.4×10^{-2}	3.2×10	-7.0×10^{-3}	5.4

($\tilde{a}\tilde{B}+\tilde{\eta}\tilde{C}$) is an order of magnitude smaller than either ($\tilde{a}+\tilde{B}$) or ($\tilde{B}+\tilde{\chi}$). Computations have been carried out for 27.5 km (not shown here) where $\tilde{B}$ and $\tilde{C}$ are much smaller, but $\tilde{\chi}$ is about the same as it is at 30 km, and these yield results quantitatively similar to those shown in Fig. 2. Hence we may conclude that the terms proportional to ($\tilde{a}\tilde{B}+\tilde{\eta}\tilde{C}$) are qualitatively unimportant at lower levels, and that the advection of ozone and Newtonian cooling can account for the features seen in Fig. 2. As may be seen in Eq. (49), these two mechanisms behave in different manners and this, in turn, leads to the complexity of Fig. 2. The situation at 52.5 km turns out to be much simpler. Here $\tilde{\chi}$ is sufficiently small to be negligible. Also, the time scale for the disturbances, τ, turns out to be such that $B\gg a$, τ^{-1} (see Fig. 7). Thus, as was shown in Section 5 of Part I, the main effect of photochemistry is to increase Newtonian cooling. In effect, therefore, we have only one non-adiabatic mechanism—Newtonian cooling—in operation, and this gives rise to the relative simplicity of Fig. 3. A comment should be made on something not shown in Figs. 2 and 3.

This is to the effect that in the presence of photochemistry and radiative transfer, the solutions on the stable side of the curve Im(ξ)=0 are genuinely stable (i.e., exponentially decaying) in contrast with the adiabatic situation where they are neutrally stable.

When several modes are unstable, one heuristically expects that the most unstable mode will dominate the situation. It is, therefore, of interest to study the properties of the solution at each value of $\tilde{U}$ [or (dU/dz)] with the greatest growth rate [or max Im(ξ) approximately]. In Figs. 4 and 5 we show max [Im(ξ)] as well as the corresponding value of Re(ξ) (non-dimensional phase speed relative to mean zonal flow) and $\tilde{\alpha}$ (non-dimensional wave number) as functions of $\tilde{U}^2$ at 30 km and 52.5 km, respectively. At 30 km we see that there is a distinct difference between the most unstable disturbances at low and high shears (or $\tilde{U}^2$); at low shears the most unstable disturbances have a small phase speed relative to the mean flow, while at higher $\tilde{U}^2$ there is a much larger negative phase speed. Also, low shear disturbances have a larger wave number than high shear disturbances. No such differences between low and high shear disturbances are found at 52.5 km. The reason for this particular difference between the two levels has already been discussed. There is another difference between the two levels. We see in Fig. 4 that

the curve of max[Im(ξ)] at 30 km for the non-adiabatic case merges with the curve for the adiabatic case for $\tilde{U}^2$ slightly greater than unity. This merging does not occur at 52.5 km until we reach values of $\tilde{U}^2$ greater than those shown in Fig. 5. The reason for the merging is that above some $\tilde{U}^2$ the time scale for the disturbance is much shorter than the photochemical and radiative time scales and hence the situation becomes approximately adiabatic. The value of $\tilde{U}^2$ at which this occurs is greater at 52.5 km because the photochemical time scales at this level are much shorter.

Figs. 4 and 5 together with Table 1 and Eq. (50) may be used to obtain the stability properties of our medium in terms of dimensional quantities. This has been done, and in Figs. 6 and 7 we show, for the most unstable solutions, $\tau[\mathrm{Im}(\alpha\xi)]^{-1}$ (the time for a disturbance to grow to e times its original amplitude), Re(ξ) (the phase speed of the disturbance relative to $\tilde{U}$), and $\lambda(2\pi/\alpha$, the wavelength of the disturbance) as functions of the shear ($|dU/dz|$) for 30 km and 52.5 km, respectively.

Observed winter shears in the stratosphere-mesosphere are typically of the order of from 3–7 m sec^{-1} km^{-1} (Batten, 1961). Thus, we see from Fig. 6, that in the neighborhood of 30 km, for observed shears, we have moderately slowly growing unstable waves with the growth rate varying from about (50 days)$^{-1}$ for $(dU/dz)=3$ m sec^{-1} km^{-1} to about (10 days)$^{-1}$ for $(dU/dz)=7$ m sec^{-1} km^{-1}. For $(dU/dz)>7$ m sec^{-1} km^{-1}, the growth rate continues to increase markedly. As we have already seen, the nature of the most rapidly growing waves for shears above and below about 6 m sec^{-1} km^{-1} appears to be distinctly different. For the smaller shears, the phase speed of the waves is small (~ -2 m sec^{-1}) and hence, the waves moves with approximately the mean value of the zonal velocity. Also, the wavelength of these waves is of the order of 5000 km. For the greater shears, the phase speed of the most rapidly growing waves is of the order of -20 m sec^{-1} [$+20$ m sec^{-1} is approximately the mean zonal velocity at 30 km (Batten, 1961)] and hence these waves might appear almost stationary. Also, their wavelength, which is of the order of 10,000 km, is about twice the wavelength of the waves at the lower shears.

From Fig. 7 we see that in the neighborhood of 52.5 km, for observed shears, we have unstable waves whose growth rates are, in general, greater than the growth rates of waves at 30 km, varying from about (50 days)$^{-1}$ for $(dU/dz)=3$ m sec^{-1} km^{-1} to (1.8 days)$^{-1}$ for $(dU/dz)=6$ m sec^{-1} km^{-1}. This is, to a large extent, due to the reduced static stability at the higher altitude. At 52.5 km, there is also no marked difference in the nature of the unstable waves for high and low shears. In both cases the most unstable waves have phase speeds of the order of -20 m sec^{-1} with respect to $\tilde{U}$. In view of the higher zonal velocities at this altitude (Batten, 1961), the waves will not appear stationary. The wavelength of the waves is of the order of 7900 km.

6. Additional remarks

The calculations in this Part have shown that as a result of photochemistry and radiative transfer, the stratosphere-mesosphere should always be unstable with respect to baroclinic waves; only for fairly high shears, however, will the growth rates for disturbances be very high. A detailed observational check of our conclusions for all levels is not, at the moment, possible. Nevertheless, the existence of baroclinic-type instabilities in the stratosphere seems certain. The analysis of the 1957 stratospheric sudden warming by Reed *et al.* (1963) shows that this disturbance involved the conversion of potential to kinetic energy typical of baroclinic instability. This warming was, furthermore, approximately stationary and of wave number two in agreement with the high shear mode of Fig. 6. Boville *et al.* (1961) have reported a weak disturbance of the stratosphere which appears to be baroclinic, and which furthermore, resembles the low shear disturbances of Fig. 6 with respect to phase speed and wavelength. Similar observations at 52.5 km are still lacking.

Of course, one does not expect observations to give detailed quantitative confirmation of the results of our highly simplified calculations. The omission of horizonal shears and other latitude variations (such as the length of the day), the simplified nature of our lower boundary condition, and the use of the two-level approximation all have undoubtedly introduced errors into our results, and the correction of these features is a matter of importance. There is also the matter of the source of the disturbance. While this matter is usually neglected in stability studies, the correlations between sudden warmings and tropospheric phenomena (Reed *et al.*, 1963) suggests that this aspect is also important. A theoretical model for this coupling based on the reflection of light from clouds is presented in Lindzen (1965).

Nevertheless, the calculations in this paper do imply that the non-adiabatic processes, radiative transfer and photochemistry of ozone, could be the destabilizing mechanisms accounting for the observed baroclinic instabilities in the stratosphere. They are, in any case, important factors in the behavior of the stratosphere-mesosphere and not to be neglected in subsequent calculations.

Acknowledgments. The author is indebted to the National Science Foundation for support of this work under Grants G 24903 at Harvard University and G 2282 at the University of Washington. Prof. R. M. Goody's interest and help in the preparation of the manuscript is appreciated. The author also wishes to thank Prof. R. J. Reed for his valuable comments.

REFERENCES

Batten, E. S., 1961: Wind systems in the mesosphere and lower ionosphere. *J. Meteor.*, **18**, 283–291.

Boville, B. W., C. V. Wilson and F. K. Hare 1961: Baroclinic waves of the polar night vortex. *J. Meteor.*, **18**, 567–580.

Burger, A. P., 1962: On the non-existence of critical wavelengths in a continuous baroclinic stability problem. *J. Atmos. Sci.*, **19**, 31–38.

Charney, J. G., 1947: The dynamics of long waves in a baroclinic westerly current. *J. Meteor.*, **4**, 135–162.

Eady, E. S., 1949: Long waves and cyclone waves. *Tellus*, **1**, 258–277.

Householder, A. S., 1953: *Principles of Numerical Analysis*. New York, McGraw-Hill Book Co., Inc., 274 pp.

Kuo, H. L., 1953: The stability properties and structure of disturbances in a baroclinic atmosphere. *J. Meteor.*, **10**, 235–243.

Lindzen, R. S., 1964: Radiative and photochemical processes in strato- and mesospheric dynamics. Ph.D. thesis, Harvard University, 210 pp.

——, 1965: The radiative-photochemical response of the mesosphere to fluctuations in radiation. *J. Atmos. Sci.*, **22**, 469–478.

Phillips, N. A., 1956: The general circulation of the atmosphere: a numerical experiment. *Quart. J. R. Meteor. Soc.*, **82**, 123–164.

——, 1963: Geostrophic motion. *Rev. Geophys.*, **1**, 123–176.

Reed, R. J., J. L. Wolfe and H. Nishimoto, 1963: A spectral analysis of the energetics of the stratospheric sudden warming of early 1957. *J. Atmos. Sci.*, **20**, 256–275.

Rossby, C. G., and collaborators, 1939: Relation between variations in the intensity of the zonal circulation of the atmosphere and the displacements of the semi-permanent centers of action. *J. Mar. Res.*, **2**, 38–55.

Thompson, P. D., 1961: *Numerical Weather Analysis and Prediction*. New York, Macmillan, 170 pp.